Long-Range Saturation of Spatial Decoherence in Wave-Field Transport in Random Multiple-Scattering Media

Chung-Chieh Cheng and M. G. Raymer

Oregon Center for Optics and Department of Physics, University of Oregon, Eugene, Oregon 97403

(Received 2 February 1999)

The transverse spatial coherence of an optical beam alters as the light traverses a dense, multiple-scattering, random dielectric medium. Results of measurements show the predicted initial increase of the decoherence (or decorrelation) rate with spatial separation, followed by saturation at large separation. This behavior can be modeled by using a Boltzmann-like transport equation for the Wigner function of the wave field, whereas the standard model for decoherence (developed for quantum wave fields), which is based on the Fokker-Planck phase-space diffusion equation, contains no saturation and fails at all separations to describe the observed behavior. [S0031-9007(99)09323-0]

PACS numbers: 42.25.Dd, 42.25.Kb

The transport of wave fields, including classical optical or acoustic waves and quantum matter waves, in random, multiple-scattering media arises in many contexts [1–4]. The degree of coherence of the wave field plays a key role in determining its energy flow. In quantum physics a certain class of coherence-reducing mechanisms is labeled "decoherence", which has been defined to be the environment-induced evolution of the (reduced) density matrix of a smaller system toward diagonality in a preferred basis on a much shorter time scale than that of evolution toward an equilibrium state [5–11]. The density matrix of a Schrödinger matter wave field $\psi(\vec{r}, t)$ is defined, in the position representation, as

$$\rho(\vec{r}, \vec{r}', t) = \langle \psi(\vec{r}, t)\psi^*(\vec{r}', t) \rangle , \tag{1}$$

where $\vec{r} = (x, y, z)$ and the bracket indicates an ensemble average over the possible forms of $\psi(\vec{r}, t)$, each being associated with a particular configuration of the environment subject to spatial or temporal fluctuations.

A simple (linear, nonlocal) model of system-environment coupling [5–9] leads to the prediction $\rho(\vec{r}, \vec{r}', t) = \rho(\vec{r}, \vec{r}', 0) \exp\{-[\gamma + R(\vec{r}, \vec{r}')]t\}$, where γ is the diagonal (energy) damping rate and

$$R(\vec{r}, \vec{r}') = \Lambda \, | \, \vec{r} - \vec{r}' \, |^2 \tag{2}$$

is the decoherence rate (with Λ being the rate of momentum diffusion). We refer to Eq. (2) as the "standard lore" [11]. The results of the first experiment measuring quantum decoherence as defined in the above sense are consistent with Eq. (2) for short times and small separations [12]. Inspired by the quantum theory, we can infer an analogous classical theory for the propagation of a scalar wave in a random medium. Here decoherence, or "decorrelation," predicts the rate at which the coherence of a wave is destroyed during propagation.

In classical optics the loss of spatial coherence through random scattering has been extensively studied [2–4,13]. For weakly depolarizing scattering processes, one can treat the electric field as a scalar wave $\psi(\vec{x}_\perp; z, t)$, where, in a beamlike geometry, z is the propagation direction and $\vec{x}_\perp = (x, y)$ is the transverse position of a point on the wave front. The spatial coherence function (SCF) of the wave field is defined as $\rho(\vec{x}_\perp, \vec{x}'_\perp; z, t) = \langle \psi(\vec{x}_\perp; z, t)\psi^*(\vec{x}'_\perp; z, t) \rangle$. Simple consideration of a two-beam interferometer shows that the decoherence rate cannot increase without bound, as implied in Eq. (2). Rather, the decoherence rate should saturate (become independent of the spatial separation between two field points) beyond a certain spatial scale set by the characteristics of the random medium causing the decoherence [10,11], and the maximum of the decoherence rate depends on the column length of the random medium traversed (i.e., the transit time through the medium). We present a theoretical and experimental examination of this saturation behavior and demonstrate the importance of the detailed nature of scattering.

A Boltzmann-like transport equation for the Wigner function of the light can accurately model the evolution of the SCF of light traversing a random medium [3,4]. This represents a generalization of the simple decoherence model based on the Fokker-Planck phase-space diffusion equation [5–9]. A transverse Wigner function (WF) of the wave field can be defined as

$$W(\vec{x}_\perp, \vec{k}_\perp; z, t) = \iint \frac{d^2\vec{s}_\perp}{(2\pi)^2} \exp(-i\vec{s}_\perp \cdot \vec{k}_\perp) \rho(\vec{x}_\perp + \vec{s}_\perp/2, \vec{x}_\perp - \vec{s}_\perp/2; z, t) , \tag{3}$$

where $\vec{k}_\perp = (k_x, k_y)$ has the interpretation of a transverse wave vector. For light propagating in a multiple-scattering medium, we can separate the transverse WF into a narrow, near-forward-propagating part W_N (defined by being within the collection solid angle Ω_N of the optical system used) and a wide-angle-scattered part W_W (which is outside Ω_N); $W = W_N + W_W$. As long as the WF varies little over an optical wavelength, the near-forward part W_N obeys [4]

$$(\partial_t + v\partial_z + \alpha\vec{k}_\perp \cdot \nabla_{\vec{x}\perp})W_N(\vec{x}_\perp, \vec{k}_\perp; z, t) = \iint d^2\vec{k}'_\perp \tilde{K}_N(\vec{k}_\perp - \vec{k}'_\perp)W_N(\vec{x}_\perp, \vec{k}'_\perp; z, t), \quad (4)$$

where $\alpha = v/k = c^2/n_0^2\omega$ for quasimonochromatic, classical light with frequency ω, velocity $v = c/n_0$, and wave-vector modulus k, in a medium with refractive index n_0. The WF is a quasi-phase-space density and contains information about wave-coherence properties absent in the ordinary Boltzmann transport equation. The scattering kernel $\tilde{K}_N(\vec{k}_\perp - \vec{k}'_\perp)$, which we consider to be strongly peaked in the forward direction, is determined by the differential scattering cross section $d\sigma/d\Omega$ of a single scatterer inside the medium,

$$\tilde{K}_N(\Delta\vec{k}_\perp) = -v\mu_T\delta^2(\Delta\vec{k}_\perp) + \alpha\frac{N}{k}\left(\frac{d\sigma(\theta)}{d\Omega}\right)_N, \quad (5)$$

where the subscript N on $d\sigma/d\Omega$ indicates only that portion of scattering within the collection angle Ω_N. The total extinction coefficient is $\mu_T = N(\sigma_A + \sigma_W + \sigma_N)$, with N being the number density of scatterers and $\sigma_W(\sigma_N)$ being the cross section for scattering into wide (near-forward) angles, distinguished by being outside (within) Ω_N. The total scattering cross section is $\sigma_S(= \sigma_N + \sigma_W)$. Other attenuation mechanisms, such as absorption, are represented by σ_A.

The corresponding equation of motion for the near-forward part of the transverse SCF, $\rho_N(\vec{x}_\perp, \vec{x}'_\perp; z, t)$, can be derived from Eqs. (3)–(5) (see also Refs. [2,10]):

$$[\partial_t + v\partial_z]\rho_N(\vec{x}_\perp, \vec{x}'_\perp; z, t) = [(i\alpha/2)(\nabla^2_{\vec{x}_\perp} - \nabla^2_{\vec{x}'_\perp}) - F(\vec{x}_\perp, \vec{x}'_\perp)]\rho_N(\vec{x}_\perp, \vec{x}'_\perp; z, t), \quad (6)$$

where

$$F(\vec{x}_\perp, \vec{x}'_\perp) = v\mu_T - vNS(\vec{x}_\perp - \vec{x}'_\perp) \equiv F(\Delta\vec{x}_\perp), \qquad S(\Delta\vec{x}_\perp) = \frac{1}{k^2}\iint_{\Omega_N} d^2(\Delta\vec{k}_\perp)\left(\frac{d\sigma(\theta)}{d\Omega}\right)_N \exp[i\Delta\vec{x}_\perp \cdot \Delta\vec{k}_\perp], \quad (7)$$

with the limiting values $S(|\Delta\vec{x}_\perp| = 0) = \sigma_N$, $S(|\Delta\vec{x}_\perp| \to \infty) = 0$. Thus the decoherence rate is predicted to increase from a value $F(|\Delta\vec{x}_\perp| = 0) = vN(\sigma_A + \sigma_W)$ to a saturated value $F(|\Delta\vec{x}_\perp| \to \infty) = v\mu_T = vN(\sigma_A + \sigma_S)$.

In the Fokker-Planck approximation, the right-hand side of Eq. (4) is replaced by $\Lambda\nabla^2_{k\perp}W(\vec{x}_\perp, \vec{k}_\perp; z, t)$. This leads directly to the standard lore of a decoherence rate, namely, Eq. (2). We address the corrections to decoherence behavior that arise from the more accurate Eqs. (4)–(7).

The experimental setup is shown in Fig. 1. We shine linearly polarized, continuous-wave He-Ne laser light ($\lambda = 632.8$ nm) into a 1 mm thick medium composed of polystyrene microspheres (diameter 46 μm, index of refraction = 1.59) suspended in a solidified gelatin/water mixture ($n_0 = 1.42$) between two 1 mm thick glass plates. We analyze the light at the output face of the gelatin medium, following a linear polarizer which blocks the orthogonal polarization (containing less than 1% of the power). The ensemble average of spatial configurations defining the SCF is achieved by rapidly moving the sample transversely over a range ± 5 mm while collecting data during a long exposure time. To measure the SCF we use a lateral-shearing Sagnac interferometer [14], which we modified by adding three lenses (L) in an arrangement such that the output face of the medium is imaged onto the camera face, while optimizing the collection solid angle without distorting the optical wave front [15]. When the mirror pair (M,M) inside the triangular ring is at position A, the two counterpropagating beams are perfectly overlapped when they reach the camera. When the mirror pair (M,M) inside the triangular ring is moved from position A to (variable) position B, the two counterpropagating images are shifted from perfect overlap ($s = 0$) at the camera to lateral shears $\pm s/2$ in the x direction, creating an interference pattern,

$$I(x + s/2, x - s/2) = \langle|\psi(x + s/2)|^2\rangle + \langle|\psi(x - s/2)|^2\rangle \pm \begin{matrix}\mathrm{Re}\\ \mathrm{Im}\end{matrix} 2\langle\psi(x + s/2)\psi^*(x - s/2)\rangle, \quad (8)$$

where we take the value $y = 0$, so the recorded data is a function of x and s (along the x direction). By varying the orientations of a set of intra-ring birefringent wave plates to introduce nonreciprocal phase shifts to the two counterpropagating beams, we perform measurements at four phase values [15], which are indicated in Eq. (8) by $\pm$Re/Im, meaning plus or minus the real or imaginary parts. From these four measurements, we can remove the first two terms on the right-hand side of Eq. (8), thereby obtaining the complex SCF, the last term of Eq. (8).

The input light beam was collimated at the medium output face ($z = 0$) with a Gaussian-beam radius 140 μm (half-width at $1/e$ maximum). The (real part of the) measured SCF, $\rho_N(x + s/2, x - s/2; z)$, is shown for two scatterer volume fractions (percent by volume) in Figs. 2(a) and 2(b). (The imaginary parts are nearly zero,

as expected.) The time dependence is dropped for a steady-state field. In Fig. 2(b) the rapid loss of coherence as a function of spatial separation (shear) can be seen near $s = 0$, followed by a region of slower decrease.

To bring out the saturation behavior clearly, we determined the decoherence rate, the exponential decay rate of the SCF, from the measured data by using

$$F(x + s/2, x - s/2) = \frac{v}{z} \ln\left|\frac{\rho_N(x + s/2, x - s/2; 0)}{\rho_N(x + s/2, x - s/2; z)}\right|, \tag{9}$$

where we have restricted the variable $\vec{x}_\perp = (x, 0)$, consistent with our measurement scheme, and $z = L = 1$ mm is the medium thickness. In this steady-state situation we identify the transit time of light t as z/v, so z formally plays the same role as time in the usual quantum theory of decoherence. Figure 3 shows, for scatterer volume fraction 2%, the decoherence rate versus separation s [the result is rather insensitive to the value of x, as expected from Eq. (7), so we averaged the results over a range ± 168 μm centered at $x = 0$]. The result clearly indicates a rapid increase of F for small s, followed by the predicted saturation to a constant value at large s.

The approximate solution of Eq. (6), when the propagation distance through the medium is small such that the second derivative (diffraction) terms are negligible, is (see also [10])

$$\rho_N(\vec{x}_\perp, \vec{x}'_\perp; z) = \rho_N(\vec{x}_\perp, \vec{x}'_\perp; 0) \exp[-F(\vec{x}_\perp, \vec{x}'_\perp) z/v]. \tag{10}$$

To determine $F(\vec{x}_\perp, \vec{x}'_\perp)$ we calculate numerically the differential cross section $(d\sigma/d\Omega)_N$ versus the angle from Mie scattering theory and then evaluate Eq. (7). For 46 μm diam spheres we find that the $1/e$ angular half-width of the forward lobe of the differential cross section is 5.8 mrad, $\sigma_S = 3.47 \times 10^{-5}$ cm^2, and $\sigma_N = 0.68\sigma_S$, which is determined by the collection solid angle of the optical system [16]. A contribution corresponding to 4% reflection from each glass plate holding the medium was included in σ_A. Good agreement (within experimental errors) is found between experiment and theory (see Fig. 3). The sharp cusp at $s = 0$ arises from the contribution of the differential cross section $d\sigma(\theta)/d\Omega$ at angles outside the forward lobe but within the collection angle, where $d\sigma(\theta)/d\Omega$ is small and oscillates as θ varies.

In, conclusion, when a wave field traverses a random, multiple-scattering medium the decrease of its transverse spatial coherence can be characterized by a rate of decoherence. Our results show the normally expected growth of the decoherence rate for small separations, followed by saturation. Interestingly, the standard quantum theory of decoherence [Eq. (2)], based on a Fokker-Planck phase-space diffusion equation, fails at all length scales to describe the behavior—at large scale it fails to include the saturation, and at small scale it fails to describe the detailed behavior of the decoherence rate, which depends on the differential cross section of the scatterers. In contrast, an evolution model based on a Boltzmann-like transport equation for the Wigner function and Mie scattering describes the results very well. The only other experimental test to date of Eq. (4) measured a smoothed WF [4], which alone cannot determine the SCF.

The transport equation embodies the idea that it is the nondiffusive nature of scattering in momentum space

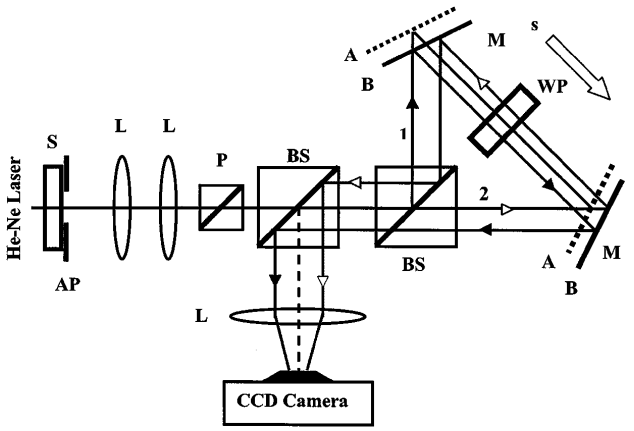

FIG. 1. Laser light passes through the scattering medium (S) whose output face is imaged using three lenses onto a charge-coupled device (CCD) camera. The output light enters the interferometer (BS = nonpolarizing 50/50 beam splitters), which measures the SCF of the transmitted light. M, mirror; P, polarizer; L, lens; AP, 1 mm aperture; WP, wave plate set.

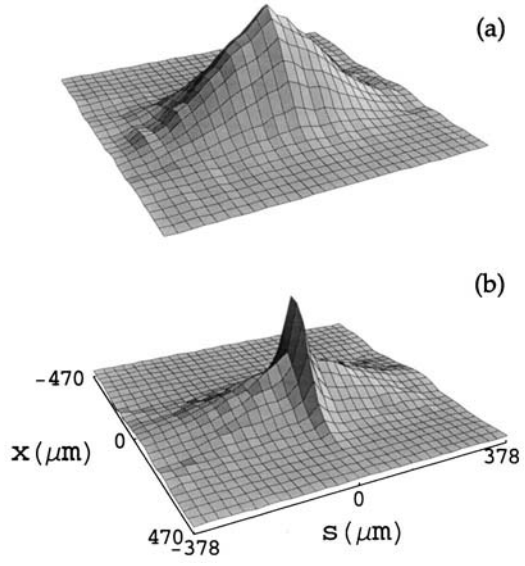

FIG. 2. Measured SCF, $\langle\psi(x + s/2)\psi^*(x - s/2)\rangle$, versus shear s and position x. In (a) [(b)] the volume fraction of the spheres in the medium is 0.4% (2%), corresponding to 0.27 (1.36) average scattering events.

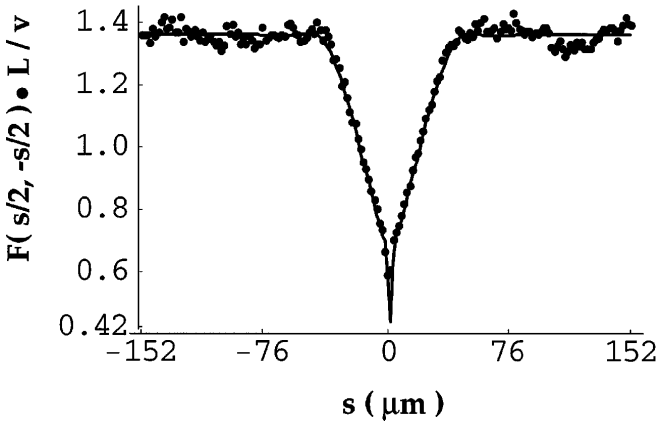

FIG. 3. Measured averaged decoherence rate times medium-transit time L/v versus separation (transverse shear) s for scatterer volume fraction 2%. Circles are measured; solid curve is theory.

which leads to the saturation of decoherence. More simply put—it is the fact that, once the two field points of interest are separated by a certain scale set by the medium, the different parts of the medium interacting with the spatial field points become uncorrelated, and further separation leads to no change of behavior [10,11]. The characteristic spatial scale is roughly the width of the Fourier transform in Eq. (7). For hard spheres, such as we use, this scale is roughly the size of the spheres, but for cold-atom collisions, for example, the characteristic scale can be much greater than the size of the scatterers.

A classical optical wave can serve as an analog for a quantum-matter wave. For quasimonochromatic (monoenergetic) waves the mathematical analogy between the two wave equations is close if the quantum field contains only single particles (say, atoms) [17,18]. Using this analogy, we were successful in predicting a means for measuring the SCF for both light waves and for atomic beams [19], and subsequently both experiments were performed and were found to be consistent [20,21].

We propose that analogous experiments can be carried out in atom optics to detect the saturation of quantum decoherence by using a diffraction-limited thermal atomic beam passing through a random scattering potential (made, for example, by using the dipole force in a standing-wave speckle pattern formed by the interference of a laser beam with its reflection from a rough surface). The transverse density matrix for the atoms can be measured using the already demonstrated method of atom-beam tomography [19,20].

We thank H. Heier for collaboration on the interferometer design, and J. Cooper and V. Shkunov for constructive criticism on the manuscript. This work is supported by the Army Research Office, and by DOE through the Oregon Medical Laser Center.

[1] A large literature exists on the transport of waves in random media. A Boltzmann equation for the Wigner function was introduced by Yu. N. Barabanenkov [Sov. Phys. JETP **29**, 679 (1969)]. Recent approaches emphasize light localization, coherent backscattering, and higher-order statistics, and are more sophisticated (and complicated) than the transport approach; for a review see Ping Sheng, *Introduction to Wave Scattering, Localization and Mesoscopic Phenomena* (Academic, San Diego, 1995). Also a large literature exists on the transport equation in the context of condensed-matter theory, where it is referred to as the quantum kinetic equation; see, for example, *Nonequilibrium Statistical Mechanics*, edited by B. C. Eu (Kluwer, Dordrecht, 1998), Chap. 9.
[2] A. Ishimaru, *Wave Propagation and Scattering in Random Media* (Academic, New York, 1978), Vols. I–II.
[3] S. John, G. Pang, and Y. Yang, J. Biomed. Opt. **1**, 180 (1996).
[4] A. Wax and J. E. Thomas, J. Opt. Soc. Am. A **15**, 1896 (1998).
[5] A. O. Caldiera and A. J. Leggett, Phys. Rev. A **31**, 1059 (1985).
[6] E. Joos and H. D. Zeh, Z. Phys. B **59**, 223 (1985).
[7] W. G. Unruh and W. H. Zurek, Phys. Rev. D **40**, 1071 (1989).
[8] W. H. Zurek, Phys. Rev. D **24**, 1516 (1981).
[9] W. H. Zurek, Phys. Rev. D **26**, 1862 (1982).
[10] M. R. Gallis and G. N. Fleming, Phys. Rev. A **42**, 38 (1990).
[11] J. R. Anglin, J. P. Paz, and W. H. Zurek, Phys. Rev. A **55**, 4041 (1997).
[12] M. Brune *et al.*, Phys. Rev. Lett. **77**, 4887 (1996).
[13] L. Mandel and E. Wolf, *Optical Coherence and Quantum Optics* (Cambridge, New York, 1995), Chaps. 4–5.
[14] C. Iaconis and I. A. Walmsley, Opt. Lett. **21**, 1783 (1996).
[15] Chung-Chieh Cheng, M. G. Raymer, and H. Heier (to be published).
[16] The collection solid angle can be written as $\Omega_N = 2\pi(1 - \cos\theta_a)$. Ray tracing our optical system to find the collection half angle θ_a yields a range of 0.10 to 0.15 rad, depending on the spatial distribution of the scatterers within the laser beam. The results of theory are not highly sensitive to the precise value used; we use $\theta_a = 0.14$ rad.
[17] I. Bialynicki-Birula, in *Progress in Optics XXXVI*, edited by E. Wolf (North-Holland, Amsterdam, 1996), p. 245.
[18] For a quantum particle of mass m, α used in Eq. (4) can be replaced by $\alpha = \hbar/m$. For multiparticle measurements the analogy may fail. See C. Brukner and A. Zeilinger, Phys. Rev. Lett. **79**, 2599 (1997).
[19] M. G. Raymer, M. Beck, and D. F. McAlister, Phys. Rev. Lett. **72**, 1137 (1994).
[20] Ch. Kurtsiefer, T. Pfau, and J. Mlynek, Nature (London) **386**, 150 (1997); M. G. Raymer, J. Mod. Opt. **44**, 2565 (1997).
[21] D. McAlister, M. Beck, L. Clarke, A. Mayer, and M. G. Raymer, Opt. Lett. **20**, 1181 (1995).